

Single Pot Synthesis of Spherical Polyaniline Stabilized AgCl Nanoparticles by Interfacial Polymerization Method and Study Its Application on Electrochemical Detection of Hydrazine and Hydrogen peroxide

K. N. Porchelvi, A. Sudarvizhi and K. Pandian*

Department of Inorganic Chemistry, University of Madras, Guindy Campus, Chennai-600 025, India

*E-mail: jeevapandian@yahoo.co.uk

Received: 2 January 2013 / Accepted: 28 January 2013 / Published: 1 March 2013

Polyaniline protected silver chloride nanoparticles based nanocomposite was synthesized by an interfacial polymerization method in which p-aminodiphenylamine was used as phase transfer agent as well as aniline source. The solid nanocomposite (AgCl@PANI) was isolated and characterized with various instrumental methods such as FT-IR, SEM, EDAX and XRD techniques to understand size and shape and the nature of functional group. The electrocatalytic behavior of the AgCl@PANI modified GCE was investigated towards the electrochemical oxidation of hydrazine in phosphate buffer medium and observed that a significant increases in peak current values at lower oxidation potential (+0.4 V vs. Ag wire). A calibration plot was constructed for the quantitative detection of hydrazine using DPV technique in the concentration ranges from 2 - 9 μM . The detection limit (3σ) for hydrazine was found to be 2.8×10^{-7} M. Similarly the electrocatalytic behaviour of polyaniline stabilised AgCl nanoparticles was also investigated on electrochemical reduction of hydrogen peroxide and shows an enhanced reduction current with lowering over potential (-0.75 V vs. Ag wire). Since the AgCl@PANI modified GCE exhibit excellent electrocatalytic oxidation and reduction behaviour for the detection of both hydrazine and hydrogen peroxide, we have compared these results with the literature reported values. Hence the proposed system can be utilised for the detection of both hydrazine and hydrogen peroxide in various environmental samples at trace level.

Keywords: Silver chloride nanoparticles, Polyaniline, Interfacial polymerization, Electrocatalytic oxidation of hydrazine, Electrocatalytic reduction of hydrogen peroxide

1. INTRODUCTION

The synthesis of a conductive nanocomposite of metal nanoparticles dispersed conducting polymers has received much attention in recent days because of their inherent optical and electronic

properties [1]. Among other conducting polymer nanocomposites, silver nanoparticles based nanocomposites were widely used in catalysis [2], conductive ink [3-5] and substrate for Raman spectral studies [6-8]. Nanocomposites derived from gold and silver nanoparticles dispersed in polyaniline are particularly important due to their excellent electrocatalytic properties [9], sensors [10] and fuel cell [11] applications. The polyaniline stabilized silver nanoparticles have been synthesized in various methods including wet chemical method [12], microemulsion route [13], interfacial polymerization [14] and electrochemical method [15]. The important advantage of the interfacial polymerization method is a slow oxidation of monomer or oligomer taken place at the interfacial of the meeting point wherein the oxidizing agent is mostly dispersed in aqueous medium whereas the respective monomer is placed in organic medium. The influence of various experimental parameters which affect the polymerization reaction such as solvent polarity, pH of the medium and addition of reaction intermediates have been investigated recently by many research groups. Recently we demonstrated a novel methodology for the synthesis of aniline oligomers such as dimer, tetramer and octamer as starting materials instead of aniline as monomer to synthesis oligoaniline or polyaniline protected metal nanocomposites [16, 17]. The purpose of using oligomer as starting material is to control the oxidation rate and is freely soluble in organic solvents. By this interfacial polymerization technique one can able to synthesis polyaniline stabilized metal nanoparticles composites with various size and shapes and high conductivity nanocomposite film.

In the present investigation, we attempted to synthesize polyaniline protected silver nanoparticle nanocomposite by interfacial polymerization method in which chemical oxidative polymerization reaction takes place at the interface where meeting point of the monomer and the aqueous AgNO_3 as oxidizing agent. Because of slow diffusion of oxidizing agent from aqueous to organic phases the oxidative polymerization occurs in a controlled manner [17]. In the present case aniline dimer is used as monomer instead of aniline because of its lower oxidation potential when compared with aniline and the silver nitrate was used as oxidizing agent without addition of any external oxidizing agent. It is well known that both aniline and dimer aniline acts as very good reducing agent [18]. The oxidative polymerizations of aniline and its oligomer using silver nitrate as oxidizing agent by an interfacial polymerization route which lead to the formation of polyaniline protected silver nanoparticles have been demonstrated recently. The present study is unique because the AgCl@PANI nanocomposite was formed under acidic medium during the addition of aqueous solution of AgNO_3 to aniline dimer in 1M HCl medium without the aid of any other chemical species. Under acidic condition the polyaniline shape was manipulated as spherical in shape instead of fibril nature of the nanocomposite as described earlier [19]. Recently a few reports are available in the literature on the synthesis of polyaniline stabilized silver chloride nanoparticles by chemical oxidative polymerization method with a complex multistage preparation procedure. Here we report a simple single pot interfacial polymerization method for the synthesis of uniform size polyaniline stabilized silver chloride nanoparticles.

It has been reported that AgCl@PANI core-shell nanocomposites were synthesized in the presence of polyvinylpyrrolidone (PVP) which was easily soluble in aqueous medium that nanocomposite modified have been utilized for the selective determination of dopamine in presence of ascorbic acid in wide ranges of pH of the medium and also such film are conductive in nature [20].

Later a similar kind of polyaniline stabilized silver chloride nanocomposite film modified electrode has been utilized for the construction of glucose oxidase biosensor for the detection of glucose in biological samples [21]. The aim of our present study is to demonstrate the application of AgCl@PANI on the electrocatalytic detection of hydrazine and hydrogen peroxide.

Hydrazine has been recognized as a neurotoxin, producing carcinogenic and mutagenic [22] effects. Due to the toxic nature of hydrazine, it induces vomiting, severe irritation in the respiratory tract and affects the central nervous system when exposed for long-term. Hence a sensitive and reliable method is required for determination of hydrazine at trace level. Many methods have been employed for the determination of hydrazine including spectrophotometry [23], fluorimetry [24], chromatography [25] and capillary electrophoresis [26]. Among these techniques, electrochemical method is found to be more efficient and simple for determination of hydrazine. Similarly the detection of hydrogen peroxide is also equally considerable, because of its great importance in the field of chemistry [27], biology [28], clinical control [29] and environmental protection [30]. Although various methods have been reported in the literature for the detection of hydrogen peroxide, the electrochemical method is considered to be simple, inexpensive and sensitive method. Here we are reporting the use of polyaniline stabilized AgCl nanoparticles modified electrode for the electrochemical detection of both hydrazine and hydrogen peroxide at trace level.

2. EXPERIMENTAL SECTION

2.1. Chemicals

All reagents used in this work were of analytical reagent grade and used as received. Aniline dimer (p-aminodiphenylamine) was obtained from Sigma Aldrich (Bangalore, India). Hydrazinium sulfate and hydrogen peroxide (30 % w/v) were received from commercial sources. Hydrochloric acid (37%) and Silver nitrate (AgNO_3) used as silver precursor, was obtained from Merck.

2.2. Instrumental Methods

2.2.1. FT-IR Spectroscopy

FT-IR spectra were recorded using a Perkin-Elmer 360 model IR double beam spectrophotometer (USA). The spectra were collected from 4000 to 400 cm^{-1} with 4 cm^{-1} resolution over 32 scans. The samples were prepared with KBr pellets.

2.2.2. Powder X-ray diffraction analysis

The X-ray diffractogram of the prepared sample (AgCl@PANI) was investigated by XRD. The XRD patterns with diffraction intensity versus 2θ were recorded in a JSO Debye Flex 2002 Seifert

diffractometer using Cu K α radiation($\lambda=1.5406 \text{ \AA}$) from 10 to 80° at a scanning speed of 1°min⁻¹. X-ray tube voltage and current were set at 40 kV and 40 mA, respectively.

2.2.3. Scanning Electron Microscopy

Scanning electron microscopy (SEM) was used to characterize the morphological and structural information of the product. This was carried out with field emission JEOL-JSM-6360 instrument, USA. In a typical measurement, a small amount of sample powder was adhered onto a copper stub using double-sided carbon tape. The sample was then sputtered with platinum to reduce charging effect. The elemental compositions of the prepared AgCl@PANI were estimated using energy dispersive X-ray (EDAX) studies.

2.2.4. Cyclic voltammeter

The CV experiment was carried out using CHI 660A electrochemical instrument, USA and Gamry model 330, USA. A three electrodes system with a single compartment cell system was used for all electrochemical studies. A platinum wire and a glassy carbon (GCE) electrode (3 mm dia) were used as counter and working electrode respectively. A silver wire is used as quasi-reference electrode whose potential was calibrated against Ag/AgCl (satd. KCl). All solutions were purged with nitrogen gas before doing all experiments. Bioanalytical system (BAS, USA) polishing kit was used to polish the GCE surface.

2.3. Preparation of AgCl@PANI

Polyaniline stabilized AgCl nanoparticles were prepared by using aniline dimer as a reducing agent at the interface of the aqueous and organic media. An aniline dimer – toluene solution was added to an aqueous 0.01M AgNO₃ solution (10 ml of 1M HCl) with 1.6:1 molar ratio of aniline dimer to AgNO₃ and the reaction mixture was allowed to stand under dark condition without stirring. After two days the organic and aqueous phase were separated and the resulting AgCl@PANI nanoparticles were isolated by centrifugation, washed many times with acetone and dried under vacuum.

2.4. Preparation of AgCl@PANI modified GCE

The surface of the GCE was cleaned first mechanically by polishing with 500 micron alumina powder, washing with DD water and then sonicated for 5 min with ethanol and DD water. Then it is dried using stream of high purity nitrogen gas. The GCE substrate was modified with a paste of AgCl@PANI suspension and then dried well at room temperature. Thus AgCl@PANI modified GCE was prepared for electrochemical experiments.

3. RESULTS AND DISCUSSION

3.1. Synthesis and characterization of polyaniline stabilized AgCl nanoparticles

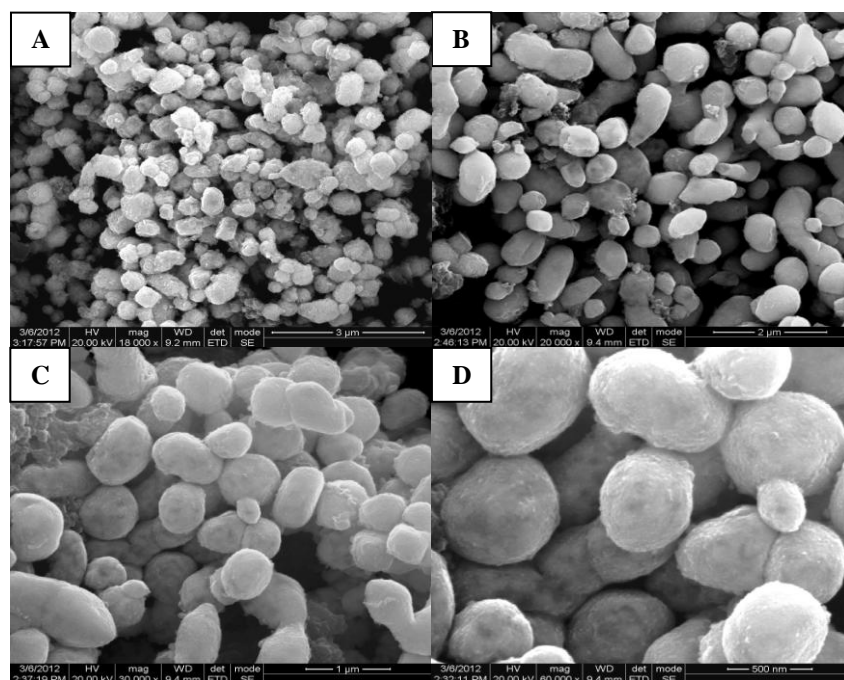


Figure 1. SEM images of polyaniline protected silver chloride nanoparticles with different magnification.

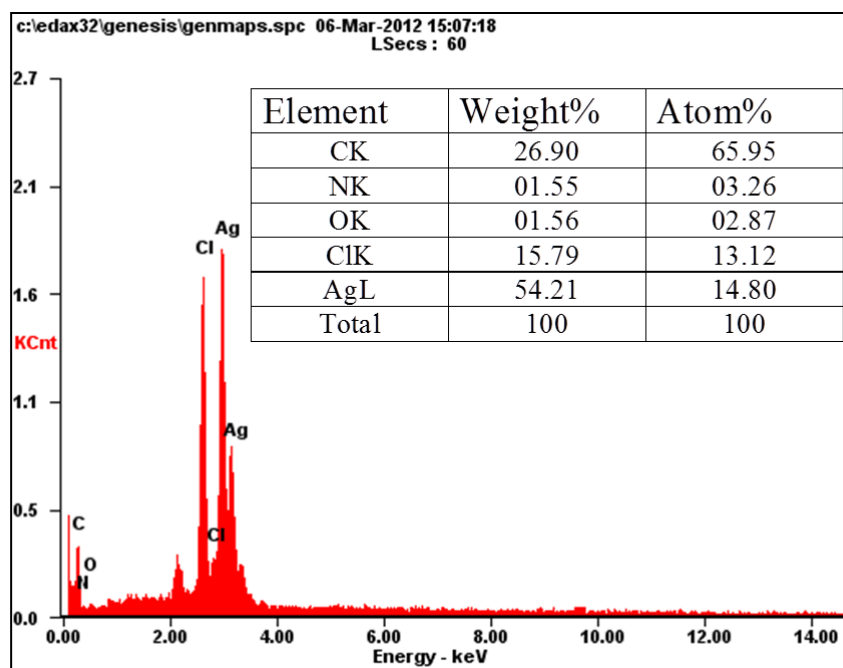


Figure 2. EDAX spectrum of polyaniline protected silver chloride nanoparticles.

A typical SEM image of the AgCl@PANI is shown in Fig.1 in which the product exhibits a spherical shape with size ranging from 100 to 200 nm. The presence of each element in AgCl@PANI samples was examined by using EDAX. The resulting graph was shown in Fig.2 and from the EDAX analysis the percentage composition of each element can be calculated. The XRD pattern of the polyaniline stabilized silver chloride nanoparticles is shown in Fig.3.

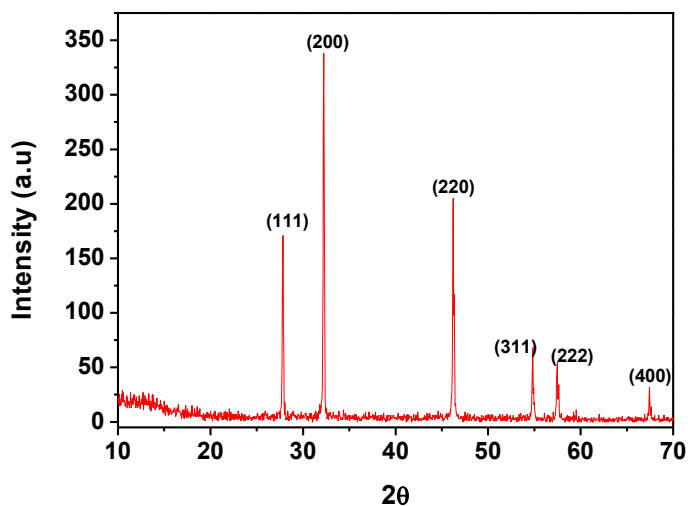


Figure 3. XRD pattern of polyaniline protected AgCl nanoparticles

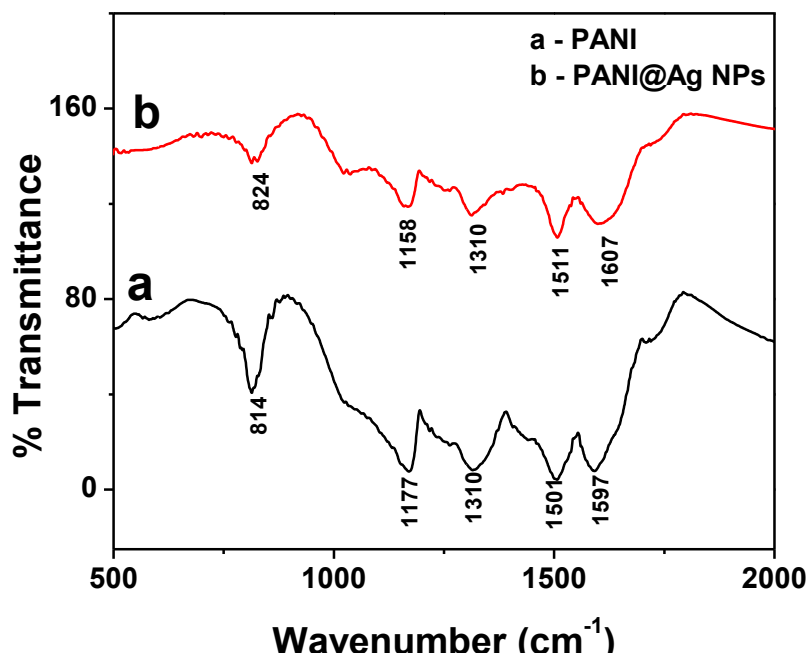


Figure 4. FT-IR spectrum of polyaniline protected AgCl nanoparticles

As shown the broad band at 2θ value of 25° peaks corresponds to the polymer chain of PANI [31]. Other peaks with 2θ values of 27.83° , 32.21° , 46.28° , 54.86° , 57.52° and 67.68° corresponds to

Bragg's reflection from (111), (200), (220), (311), (222) and (400) of AgCl. The XRD pattern of AgCl@PANI system is exactly matching with the XRD pattern of AgCl reported in the literature (JCPDS File No. 06-0480). Instead of getting the broad XRD pattern for the nanocrystalline silver chloride we observed a narrow line shaped peaks which could be due to the bigger size silver chloride particles present in the nanocomposite. The FT-IR spectrum of AgCl@PANI is shown in Fig. 4. The broad peak around 3469 cm^{-1} shows the N-H stretching of benzenoid ring present in the polyaniline backbone whereas the bands at 1597 and 1511 cm^{-1} are attributed to C=N and C=C stretching mode of vibration for the quinonoid and benzenoid units of PANI. The peak at 1158 cm^{-1} shows the combination modes of benzenoid and quinonoid unit. The peak at 1310 cm^{-1} is assigned for the C-N stretching of PANI [32]. A sharp peak at 819 cm^{-1} is assigned to C-H out of the plane bending of the para substituted benzene rings. For a comparison, the FT-IR spectrum of pure PANI which was synthesised by chemical oxidative polymerization method and AgCl@PANI were presented in a single graph.

3.2. Electrochemical behaviour of AgCl@PANI nanocomposite

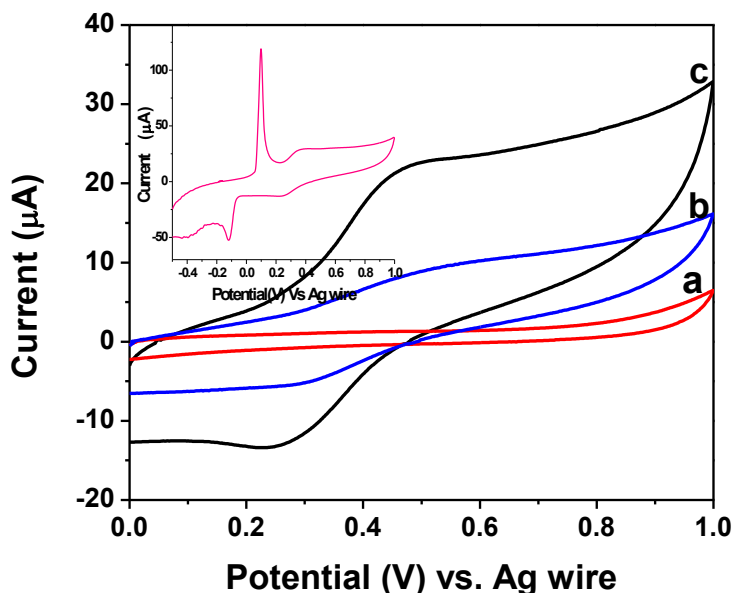


Figure 5. Cyclic Voltammogram of (a) bare (b) Hz/GCE (c) Hz/AgCl@PANI/GCE in 0.1 M Phosphate buffer solution (pH 7.5) at a scan rate of 50 mV/s. Inset shows the cyclic voltammogram of AgCl@PANI in 0.1M Phosphate buffer solution at a scan rate of 50 mVs^{-1} .

The electrochemical behaviour of polyaniline stabilized AgCl nanoparticles is carried out using 0.1M phosphate buffer solution and the resulting CV response is shown in Fig. 5 (inset Fig). A reduction peak was observed at -0.11 V vs. Ag wire whereas two oxidation peaks ($E_{\text{pa}}(\text{I})$ and $E_{\text{pa}}(\text{II})$) were observed during the reverse scan. The peak potential of $+0.09\text{ V}$ vs. Ag wire is assigned for the oxidation of the zero valent silver nanoparticles (Ag (0) to Ag (I)). The results are consistent with the literature reported results [33]. The cyclic voltammogram was recorded at various scan rates under

identical experimental conditions. The electrocatalytic oxidation and reduction behavior of the AgCl@PANI nanocomposite is described in the following paragraphs.

3.3. Electrocatalytic oxidation of Hydrazine

The electrocatalytic behaviour of polyaniline stabilized silver nanoparticles was tested towards the electrocatalytic oxidation of hydrazine. Since silver nanoparticles have shown enhanced activity towards oxidation of hydrazine recently, we have utilized the polyaniline stabilized silver chloride nanoparticles for the electrochemical oxidation of hydrazine.

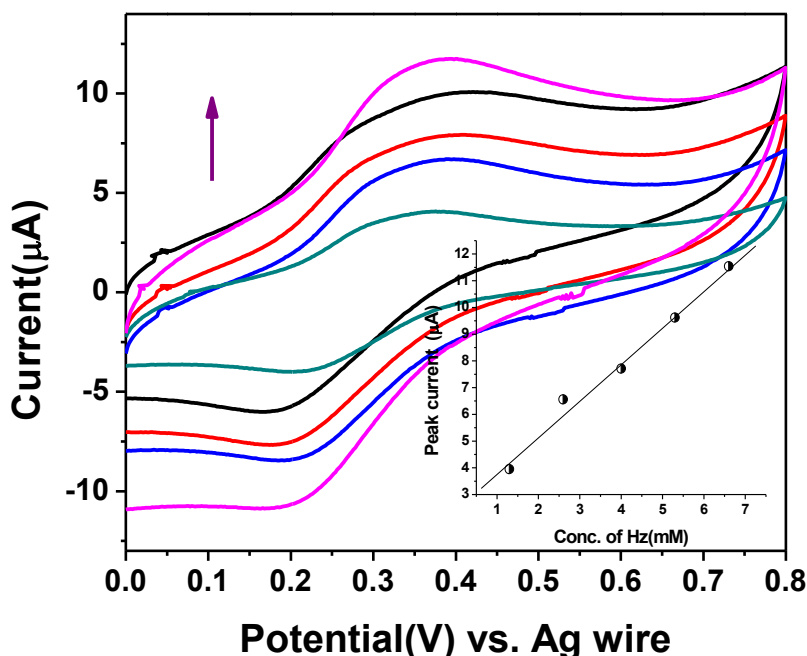
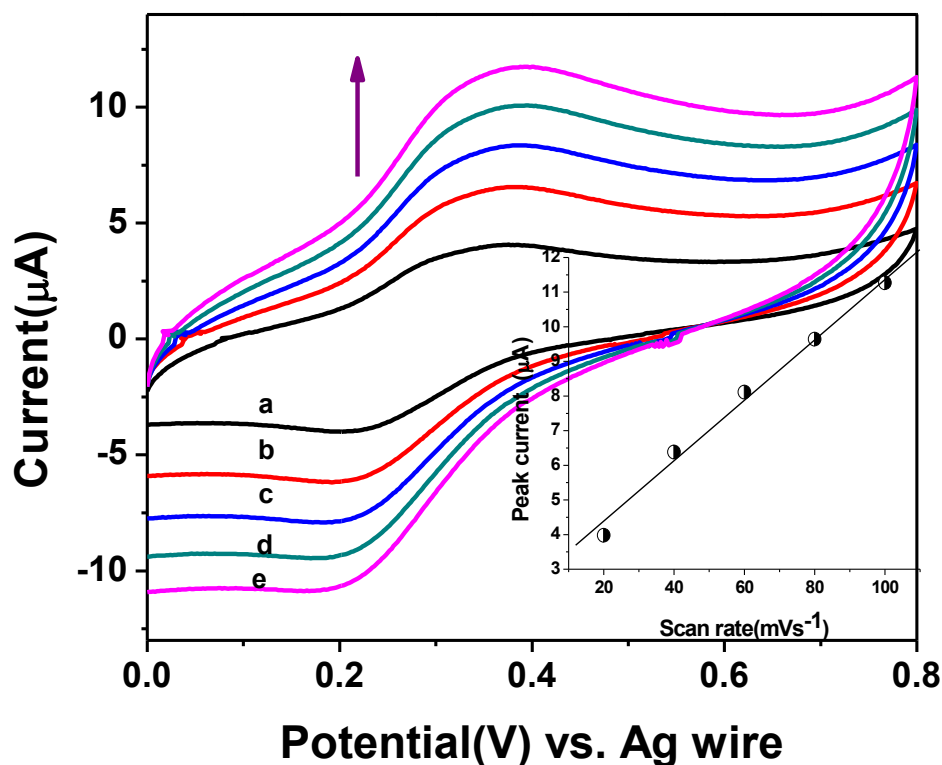


Figure 6. The effect of concentration on electrochemical oxidation of hydrazine (1.3 – 6.6mM) on AgCl@PANI modified GCE in N_2 saturated 0.1 M Phosphate buffer solution at a scan rate of 50 mVs^{-1} . Inset shows the plot of anodic peak current against concentration of hydrazine.

As shown in Fig 6 the oxidation peak was observed at +0.48V vs. Ag wire when the addition of hydrazine to the electrolyte solution. Compared to bare GCE, the peak current increased abruptly for oxidation of hydrazine when AgCl@PANI modified GCE was used. This is due to the facile electron transfer reaction taking place when the electrode is modified with AgCl@PANI. Hence these kind of modified electrodes are used for the trace level detection of hydrazine present in various sources. Fig. 6 shows the cyclic voltammogram for the electrocatalytic oxidation of hydrazine at AgCl@PANI modified GCE for various concentrations of hydrazine (20 – 100 μL). The graph shows the calibration plot for peak current against the concentration of hydrazine. A linear response was observed in the concentration range of 1.3 – 6.6 mM of hydrazine with linear correlation coefficient of 0.985. Table 1 provides detailed information about the comparison data for the present data with all recently reported literature results.

Table 1. Comparison of electrocatalytic detection of hydrazine with various types of modified electrode systems.

| Electrode System | pH | Conc. Ranges | Detection limit | Ref. |
|------------------------------|------|--------------------------|-------------------------------|--------------|
| Pd/CILE | 7.0 | 5 – 800 μM | 0.82 μM | 34 |
| ZnO | 7.0 | 0.1 - 1 μM | 147.54 nM. | 35 |
| ZnO/MWCNT | 7.4 | 0.5 – 1800 μM | 0.15 μM | 36 |
| CoHCF@TNT | 6.9 | 0.5 - 2.5 mM | $1 \times 10^{-3} \text{M}$ | 37 |
| CeHCF/Mesoporous Carbon | 1.5 | 1 - 163 μM | - | 38 |
| Ni(II)-bicaein complex/MWCNT | 13.0 | 0.2 - 2.5 mM | 0.8 μM | 39 |
| CFA/GCE | 7.5 | 0.01 - 2.0 mM | 0.4 μM | 40 |
| NiHCF@TiO ₂ NPs | 8.0 | 0.2 - 1 μM | $1.1 \times 10^{-7} \text{M}$ | 41 |
| AgCl@PANI/GCE | 7.5 | 2 - 9 μM | $2.8 \times 10^{-7} \text{M}$ | Present work |

**Figure 7.** The effect of scan rate on electrochemical oxidation of hydrazine on AgCl@PANI modified GCE in N₂ saturated 0.1M Phosphate buffer solution (pH 7.5) at different scan rates (20 - 100 mVs^{-1}). Inset shows the plot of anodic peak current against different scan rates.

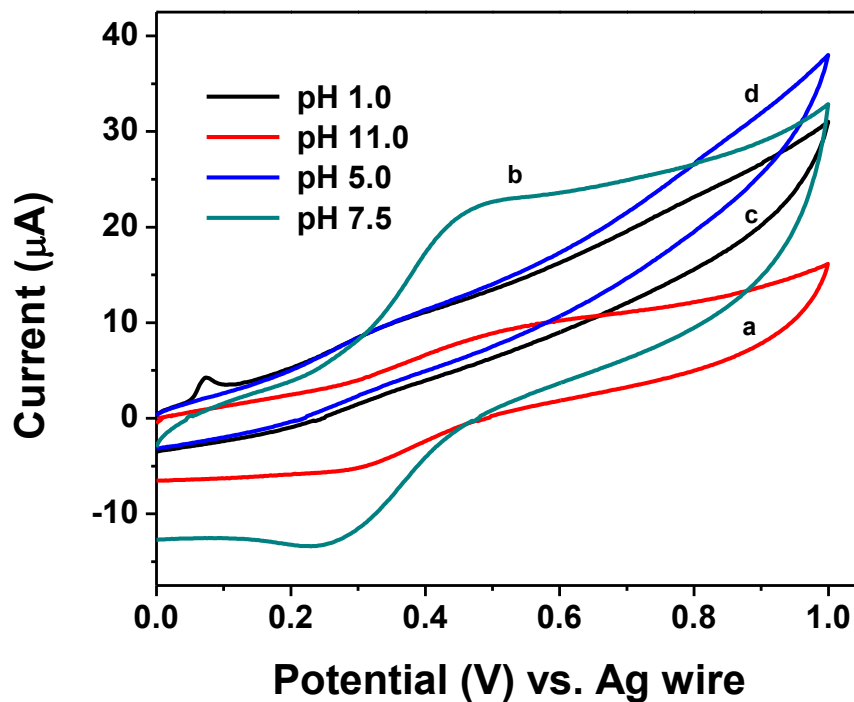


Figure 8. The electrochemical oxidation of hydrazine on AgCl@PANI modified GCE in N₂ saturated 0.1 M Phosphate buffer solution (pH 7.5) at different pH ((a) 11.0 (b) 7.5(c) 1.0 (d) 5.0).

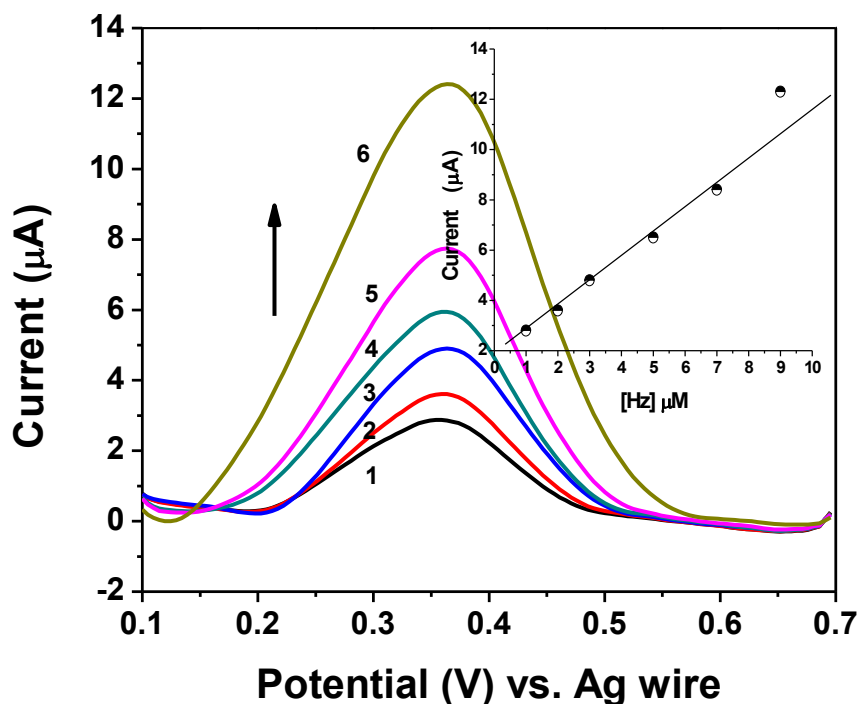


Figure 9. Differential pulse voltammograms for different concentrations of hydrazine on AgCl@PANI modified GCE in N₂ saturated 0.1 M Phosphate buffer solution (pH 8.0) containing (1).2.0, (2).3.0, (3).4.0, (4).5.0, (5).6.0 and (6).9.0 µM of Hydrazine. Inset: Plot of the peak currents as a function of concentration of hydrazine.

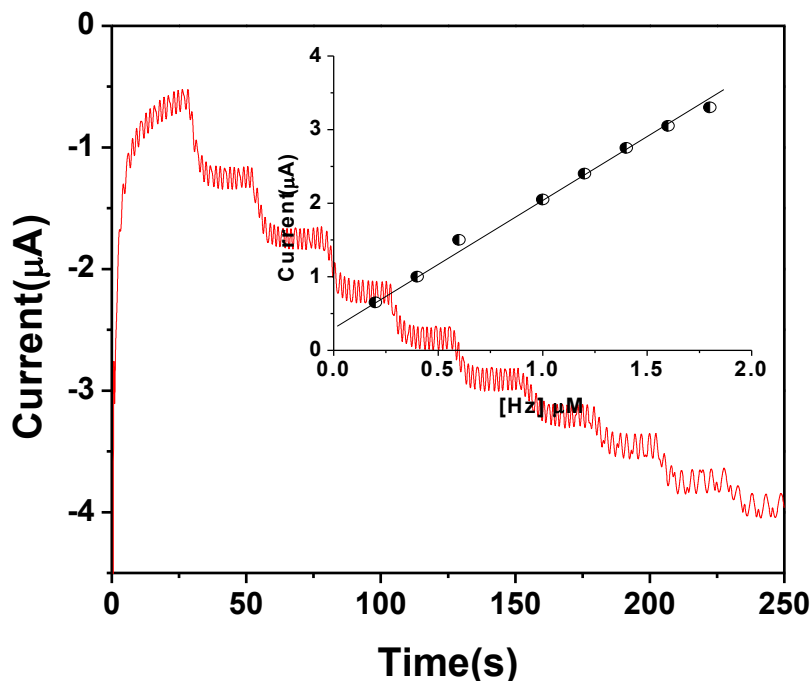


Figure 10. Amperometric behavior of hydrazine on AgCl@PANI modified GCE in 0.1M Phosphate buffer solution (pH 8.0) for successive addition of hydrazine (20µL) with an applied potential of +0.45V vs. Ag wire. Inset shows the plot of current response against the conc. of hydrazine added each time.

Differential pulse voltammetry (DPV) was used to determine the concentration of hydrazine to construct a calibration plot for the trace level detection. The voltammograms clearly showed that the plot of peak current versus hydrazine concentration constituted a linear segment with slope, corresponding to the different concentration of hydrazine from 2-9 µM as shown in Fig. 9. The detection limit (3σ) was found to be 2.8×10^{-7} M. The amperometric behaviour of hydrazine oxidation using AgCl@PANI modified GCE is shown in Fig 10. The oxidation potential was fixed at +0.45 V vs. Ag wire. The resulting current response was plotted against concentration of hydrazine and the resident time was maintained about 250 s. From the linear calibration graph and the concentration range we can exploit the system for the detection of hydrazine in various samples under identical experimental condition.

3.4. Electrocatalytic reduction of Hydrogen peroxide

The Electrocatalytic reduction behaviour of polyaniline stabilized silver nanoparticles was tested towards the electrocatalytic reduction of hydrogen peroxide. Since silver nanoparticles have been proven to be effective catalyst for detection of hydrogen peroxide, electrocatalytic reduction of hydrogen peroxide was carried out using polyaniline stabilized silver nanoparticles. Fig. 11 shows the electrocatalytic reduction of hydrogen peroxide at various concentrations and the reduction peak was observed at -0.75V vs. Ag wire. The increase in the catalytic current with respect to the added

concentration of hydrogen peroxide is due to the efficient electron transfer behavior of the AgCl@PANI nanocomposite system. The graph shows the calibration plot for peak current against the concentration of hydrogen peroxide (inset in Fig. 11).

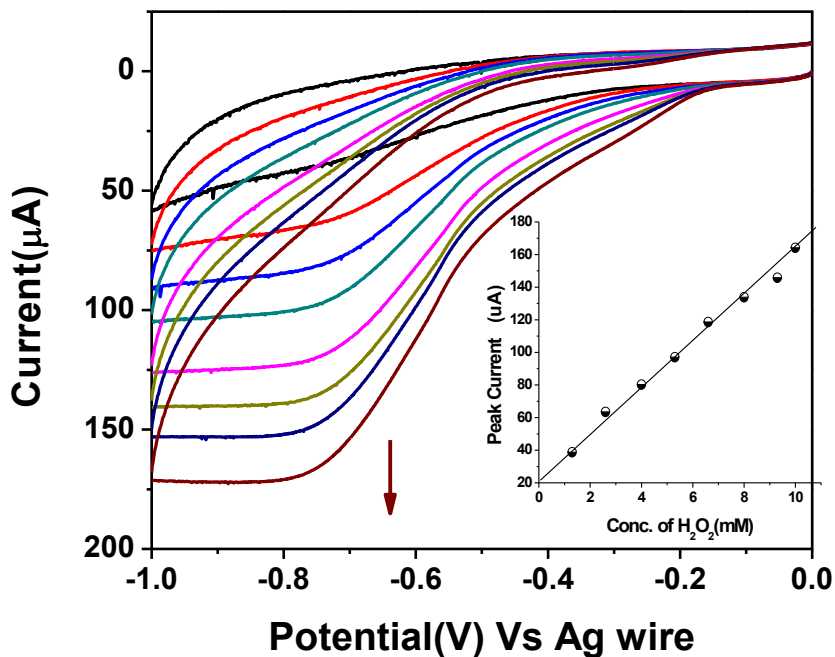


Figure 11. Cyclic Voltammogram for the electrochemical reduction of hydrogen peroxide on AgCl@PANI modified GCE in N_2 saturated 0.1 M Phosphate buffer solution (pH 7.5) at a scan rate of 50 mVs^{-1} . Inset shows the plot of cathodic peak current against concentration of hydrogen peroxide.

A linear current response was observed in the concentration ranges of 1.3–10 mM of hydrogen peroxide with a linear correlation coefficient of 0.992. Table 2 gave a comparison data with respect to the other reported literature results.

Table 2. Comparison of electrocatalytic detection of hydrogen peroxide with various types of modified electrode systems.

| Electrode | pH | Conc. Range | Detection Limit | Ref. |
|----------------------------------|------|--|--------------------------------|--------------|
| PEDOT-PB/GCE | 7.2 | $1-5 \times 10^{-5} \text{ mM}$ | - | 42 |
| Ag NP/F-SiO ₂ /GO | 6.5 | $1 \times 10^{-4} \text{ M} - 0.26 \text{ M}$ | $4 \times 10^{-6} \text{ M}$ | 43 |
| Ag nanowire | 6.5 | $20 \text{ } \mu\text{M} - 3.62 \text{ mM}$ | $2.3 \text{ } \mu\text{M}$ | 44 |
| PB@Pt ^{nano} /PCNTs/GCE | 2.0 | $1.5 \times 10^{-3} - 2.5 \times 10^{-7} \text{ } \mu\text{M}$ | $1.5 \times 10^{-7} \text{ M}$ | 45 |
| AgNP/TiO ₂ NW | 7.4 | 0.1- 60 mM | $1.70 \text{ } \mu\text{M}$ | 46 |
| Cu-rich-CuHCF/GCE | 5.5 | $3.5 \times 10^{-5} - 5 \times 10^{-7} \text{ } \mu\text{M}$ | $5 \times 10^{-7} \text{ M}$ | 47 |
| SPAgE-Bi ^{nano} | 7.0 | 0.1-5 | $56.59 \text{ } \mu\text{M}$ | 48 |
| Ag@P(mPD)-Ag | 6.5 | 0.1-170 mM | 2.5 nM | 49 |
| m-VZrO ₂ -GCE | 10.0 | 5 - 400 μM | 0.9 nM | 50 |
| AgCl@PANI/GCE | 7.5 | 1.3 – 10 mM | $1 \times 10^{-4} \text{ M}$ | Present work |

4. CONCLUSION

In summary, we have succeeded in preparation of spherical shaped polyaniline stabilized silver chloride nanoparticles through interfacial polymerization method. The formation of spherical shaped AgCl@PANI nanoparticles was confirmed with SEM, EDAX, XRD and FT-IR. The electrochemical behaviour of the AgCl@PANI nanoparticles was tested towards the electrochemical oxidation of hydrazine and reduction of hydrogen peroxide. A linear response was observed for both hydrazine and hydrogen peroxide in the concentration range of 1-9 μM to 1.3-10 mM with the linear coefficient of 0.985 and 0.992 respectively. The detection limit for hydrazine was found to be 2.8×10^{-7} M. The electrochemical behaviour of such a novel nanoparticles system is in progress in our laboratory.

ACKNOWLEDGEMENT

Financial support from UGC, New Delhi is gratefully acknowledged and the authors are expressing their gratitude to SAIF, IIT Madras for providing SEM, XRD and FT-IR facilities.

References

1. G. Schmid, *Colloids and Clusters*, VCH Press, NY (1995).
2. X.M. Feng, C.J. Mao, G. Yang, W.H. Hou and J.J. Zhu, *Langmuir*, 22 (2006) 4384.
3. RA. D. Barros, WM. D. Azevedo and FM. D. Aguiar, *Mater. Charact.*, 50 (2003) 131.
4. RA. D. Barros, CR. Martins and WM. D. Azevedo, *Synth Met.*, 35 (2005) 155.
5. H.S. Jae, I.L. Bock, M.L. Chae and C. Gyoujin, *IEEE Nanotechnology Materials and Devices Conference, NMDC.*, 1 (2006) 582.
6. R.F. Aroca, P.J.G. Goulet, D.S. dos Santos, R.A. Alvarez-Puebla and O.N. Oliveira, *Anal. Chem.*, 77 (2005) 378.
7. Y. Flegler and M. Rosenbluh, *Research Letters in Optics.*, (2009) 5 pages.
8. C. L. Haynes, A. D. McFarland and R. P. Van Duyne, *Anal. Chem.*, (2005) 338.
9. Y. Gao, D. Shan, F. Cao, J. Gong, X. Li, H. Y. Ma, Z. M. Su and L. Y. Qu, *J. Phys. Chem. C.*, 113 (2009) 15175.
10. A. Choudhury, *Sens. Actuators B.*, 138 (2009) 318.
11. F. J. Liu, L. M. Huang, T. C. Wen, K. C. Yin, J. S. Hung and A. Gopalan, *Polym Compos.*, 28 (2007) 650.
12. Y. B. Wankhede, S. B. Kondawar, S. R. Thakare and P. S. More, *Adv. Mat. Lett.*, 4 (2013) 89.
13. Z. Zhou, H. Deliang, Y. Guo, Z. Cui, M. Wang, G. Li and R. Yang, *Thin Solid Films*, 517 (2009) 6767.
14. M.M. Oliveira, E.G. Castro, C.D. Canestraro, D. Zanchet, D. Ugarte, L.S. Roman and A.J.G. Zarbin, *J. Phys. Chem. B.*, 110 (2006) 17063.
15. J. M. Kinyanjui, N. R. Wijeratne, J. Hanks and D. W. Hatchett, *Electrochim. Acta.*, 51 (2006) 2825.
16. A. N. Grace, K. Pandian, *Electrochem. Commun.*, 8 (2006) 1340.
17. P. Paulraj, N. Janaki, S. Sandhya and K. Pandian, *Colloids and Surfaces A: Physicochem. Eng. Aspects.*, 377 (2011) 28.
18. J. Song, Y. Chu, Y. Lin, L. Li, *Chem. Commun.*, (2008) 1223.
19. L. Gao, S. Lv and S. Xing, *Synth. Met.*, 162 (2012) 948.
20. W. Yan, X. Feng, X. Chen, X. Li and J. J. Zhu, *Bioelectrochemistry*, 72 (2008) 21.
21. W. Yan, X. Feng, X. Chen, W. Hou and J.J. Zhu, *Biosens. Bioelectron.*, 23 (2008) 925.

22. C. B. McAuley, C. E. Banks, A. O. Simm, T. G. J. Jones, and R. G. Compton, *Analyst*, 131 (2006) 106.
23. M. George, K. S. Nagaraja, and N. Balasubramanian, *Talanta*, 75 (2008) 27.
24. A. A. Ensafi and B. Rezaei, *Talanta*, 47 (1998) 645.
25. M. Mori, K. Tanaka, Q. Xu, M. Ikedo, H. Taoda, and W. Hu, *J. Chromatogr., A*, 1039 (2004) 135.
26. W. C. Yang, A. M. Yu, Y. Q. Dai, and H. Y. Chen, *Anal. Lett.*, 33 (2000) 3343.
27. X. Luo, J. Xu, W. Zhao and H. Chen, *Biosens. Bioelectron.*, 19 (2004) 1295.
28. Y. Wang, J. Huang, C. Zhang, J. Wei and X. Zhou, *Electroanalysis*, 10 (1998) 776.
29. X. Lu, J. Zhou, W. Lu, Q. Liu and J. Li, *Biosens. Bioelectron.*, 23 (2008) 1236.
30. X. Shu, Y. Chen, H. Yuan, S. Gao and D. Xiao, *Anal. Chem.*, 79 (2007) 3695.
31. S. K. Pillalamarri, F. D. Blum, S. T. Tokuhira, J. G. Story and M. F. Bertino, *Chem. Mater.*, 17 (2005) 227
32. S. L. Zhou, S. S. Mo, W. J. Zou, F. P. Jiang, T. X. Zhou and D. S. Yuan, *Synth. Met.*, 161(2011) 1623.
33. D. Chao, L. Cui, J. Zhang, X. Liu, Y. Li, W. Zhang, C. Wang, *Synth. Met.*, 159 (2009) 537.
34. N. Maleki, A. Safavi, E. Farjami and F. Tajabadi, *Anal. Chim. Acta.*, 611(2008) 151.
35. S. K. Mehta, K. Singh, A. Umar, G. R. Chaudhary, S. Singh, *Electrochim. Acta.*, 69 (2012) 128.
36. C. Zhang, G. Wang, Y. Ji, M. Liu, Y. Feng, Z. Zhang and B. Fang, *Sens. Actuators, B*, 150 (2010) 247.
37. S. J. Sophia, S. Devi and K. Pandian, *ISRN Anal. Chem.*, 2012 (2012) 8 pages.
38. N. R. Stradiotto, S. S. L. Castro, R. J. Mortimer and M. F. De Oliveira, *Sensors*, 8 (2008) 1950.
39. L. Zheng and J. F. Song, *Talanta*, 79 (2009) 319.
40. A. Salimi, L. Miranzadeh and R. Hallaj, *Talanta*, 75 (2008) 147.
41. S. J. Sophia, S. Devi and K. Pandian, *Int. J. Electrochem. Sci.*, 7 (2012) 6580.
42. S. Lupu, *Synth. Met.*, 161 (2011) 384.
43. Wenbo Lu, Yonglan Luo, Guohui Chang, Xuping Sun, *Biosens. Bioelectron.*, 26 (2011) 4791–4797.
44. X. Yang, J. Bai, Y. Wang, X. Jiang and X. He, *Analyst*, 137 (2012) 4362.
45. J. Zhang, J. Li, F. Yang, B. Zhang and X. Yang, *Sens. Actuators, B*, 143 (2009) 373.
46. X. Qina, W. Lua, Y. Luoa, G. Changa, A. M. Asiri, A. O. Al-Youbi, X. Suna, *Electrochim. Acta.*, 74 (2012) 275.
47. L. Guadagnini, D. Tonelli and M. Giorgetti, *Electrochim. Acta*, 55 (2010) 5036.
48. M. H. Chiu, A. S. Kumar, S. Sornambikai, P. Y. Chen, Y. Shih and J. M. Zen, *Int. J. Electrochem. Sci.* 6 (2011) 2352.
49. J. Tian, Y. Luo, H. Li, Wenbo Lu, G. Chang, *Catal. Sci. Technol.*, 1 (2011) 1393.
50. A. Domenech and J. Alarcon, *Anal. Chim. Acta.*, 452 (2002) 11.